Proceedings of 20th International Congress on Acoustics, ICA 2010

23–27 August 2010, Sydney, Australia

Hydrophone self-localisation using travel times estimated from ocean noise cross-correlations

Laura A. Brooks (1) and Peter Gerstoft (2)

(1) School of Mechanical Engineering, The University of Adelaide, Adelaide, SA, 5005 Australia
(2) Marine Physical Laboratory, Scripps Institution of Oceanography, La Jolla, California 92093-0238 USA

PACS: 43.30.Xm,43.30.Pc

ABSTRACT

Approximation of acoustic Green's functions through cross-correlation of acoustic signals in the ocean is a relatively young field that has become an area of interest over the past few years. Although the amplitudes of these estimates generally differ from those of the true Green's Function, the estimated arrival structure can be highly accurate. Inter-hydrophone travel times extracted from these Green's Function estimates can therefore be relied upon for practical applications. Acoustic data were collected for two weeks during late 2006 on an L-shaped array (combination of vertical hydrophone line array and horizontal bottom-mounted hydrophone line array) that was deployed in shallow water (70-75m depth) on the New Jersey Shelf. The data were cross-correlated and acoustic Green's Functions were subsequently estimated. This paper describes how the inter-hydrophone travel times extracted from these Green's Function estimates were used to self-localise the array. Successful implementation of this cross-correlation derived travel-time application provided the array geometry information necessary for both ambient and active source acoustic data recorded on the array to be useful for other analyses.

INTRODUCTION

The Green's function between two points is the point source solution of the governing acoustic propagation equations (i.e., it is the signal that would be received at one point given a unit impulsive source at the other). It is fully dependent upon the geometry and environment under consideration, and therefore can be used to determine information about the environment, through which acoustic transmission between the two points takes place.

It has been shown that good estimates of the acoustic Green's function between two points can be determined from cross-correlations of diffuse sound fields (Lobkis & Weaver 2001). This concept, which eliminates the requirement of having a source at either location, has been successfully applied to problems in ultrasonic noise e.g., (Weaver & Lobkis 2001, Malcolm et al. 2004, van Wijk 2006), ambient noise in a homogeneous medium (e.g., Roux et al. 2005), seismic noise (e.g., Campillo & Paul 2003, Snieder 2004, Shapiro et al. 2005, Sabra et al. 2005, Gerstoft et al. 2006, Wapenaar & Fokkema 2006, Yang et al. 2007, Lin et al. 2007), moon-seismic noise (e.g., Larose et al. 2005), and even human skeletal muscle noise (e.g., Sabra et al. 2007).

In recent years, acoustic Green's function estimates through ocean noise cross-correlation have been explained theoretically (Sabra et al. 2005), and demonstrated experimentally (Roux et al. 2004). Siderius et al. (2006) applied the concept to passive fathometry, and showed that it can be used to approximate seafloor structure. Sabra et al. (2005b) used noise cross-correlation for array localisation and self-synchronisation. These studies all concluded that accurate direct-path acoustic travel times between hydrophones can be obtained from noise cross-correlation in the ocean.

The acoustic data under consideration here were collected during late 2006 on an L-shaped array (combination of vertical hydrophone line array and horizontal bottom-mounted hydrophone line array) that was deployed in shallow water (70-75m depth) on the New Jersey Shelf. Tropical Storm Ernesto passed through the region during the array deployment. Large sea state and wind conditions developed and thus active source experimental activities were ceased; however, the acoustic hydrophone array remained operative throughout this period. The extraction of Green's function estimates from 20–100 Hz noise recorded on the horizontal portion of the hydrophone array from during this period have been discussed in detail elsewhere (Brooks & Gerstoft 2009), as has diagnosis of channel faults that occurred in the array during that period (Brooks et al. 2008). Travel times extracted from the Green's function estimates were shown to approximately match those expected for the *a priori* array geometry; however, a detailed comparison of all inter-hydrophone travel time estimates with the linear *a priori* geometry was not done.

Preliminary analysis of active source data recorded on the array before and after the passing of Tropical Storm Ernesto suggested small anomalies in the horizontal array geometry. Differences in travel times from any given active source (at a known location) to hydrophone pairs were consistently less than expected for the assumed straight-line array geometry, suggesting that the hydrophone array may not have been located linearly on the seafloor (i.e., that it is splayed). It was thus deemed necessary to either confirm or correct the *a priori* geometry of the array (i.e., localise the array) so that any acoustic data collected on the array could be confidently used for other applications.

Estimation of array shape from travel times and other acoustic data has previously been performed using discrete sources (Hodgkiss 1989, Hodgkiss et al. 2003, Dosso et al. 2004). Either an active source or ship noise at approximately known locations is used. If exact source locations are not known, the inversion algorithm can invert for both source and receiver positions. Inputs

for the inversions generally consist of source-receiver travel times, *a priori* estimates of the source and receiver geometry, and estimated errors in travel times and geometry, as well as other assumptions such as the array elements being able to be approximated by a smooth function.

Sabra et al. (2005b) developed a two-dimensional algorithm (all receivers must be located on the same horizontal plane, allowing for an isovelocity assumption) for array element self-localisation from ambient noise cross-correlations. Their methods were experimentally shown to be effective for HLA hydrophone localisation, and as such, form a basis for the methodology presented here.

Travel times extracted from day-long noise cross-correlations are used here in a hydrophone self-localisation inversion to estimate the true geometry of the horizontal portion of the L-shaped array. All the horizontal line array (HLA) elements as well as the lowest vertical line array (VLA) element are considered. The VLA element is included so that the location of the HLA relative to the VLA can be estimated also. Velocity changes near the bottom of the water column are negligible and therefore the isovelocity assumption remains valid when considering cross-correlations with the lowest VLA element. The curved array geometry estimated here provides more consistent acoustic travel times for active noise sources than the *a priori* assumed straight line geometry.

CROSS-CORRELATION THEORY

In an ocean environment it would be desirable to have a volume distribution of sources, as this would excite all acoustic modes, enabling an accurate Green's function approximation to be obtained from acoustic cross-correlations. Source configurations that do not meet this criterion will yield poorer Green's function approximations (Brooks & Gerstoft 2009).

In the absence of an active test source, acoustic fields recorded by seafloor mounted hydrophones can be dominated by shipping noise, or by ambient noise sources such as biological species or ocean waves. At frequencies above a few hundred Hertz the ocean sound field is usually dominated by surface noises from ocean waves (Wenz 1962, Urick 1975, Loewen & Melville 1991), whilst at frequencies below about 100 Hz the noise field is usually dominated by shipping noise (Wenz 1962, Urick 1975).

The noise field is here modelled as a set of sources that are uniformly and densely distributed within a horizontal plane near the surface of a waveguide. This assumption is reasonable for either ocean wave dominated fields, or ship dominated sound fields in regions of high shipping density. Although this configuration does not meet the desired volume distribution discussed previously, it is sufficient for the approximation of direct-path travel times (Brooks & Gerstoft 2009).

The cross-correlation of acoustic data recorded on two receivers in the ocean can be derived following the stationary phase methodologies of Snieder et al. (2006) and Brooks et al. (2007). The cross-correlation of the signals recorded at two receivers, A and B, is:

$$C_{AB}(\omega) = |\rho S(\omega)|^2 n \iint G(\mathbf{r}_A, \mathbf{r}_S) G^*(\mathbf{r}_B, \mathbf{r}_S) dxdy, \qquad (1)$$

where $S(\omega)$ is the ship source spectrum, ρ is the density of the medium, n is the number of sources per unit area, $G(\mathbf{r}_\psi, \mathbf{r}_S)$ is the Green's function between the source, S, and receiver, ψ, * denotes the complex conjugate, and x and y are the horizontal axes parallel and perpendicular to the vertical plane containing A and B respectively.

The full Green's function at each receiver can be written as a superposition of direct and reflected waves. For a uniform sound speed (isovelocity) waveguide, bounded by a free surface at the top and a bottom with reflection coefficient Γ (assumed to be independent of angle of incidence), the Green's function between the source, S, and receiver, ψ, can be expressed as a sum of free-field Green's functions (Brekhovskikh 1960, Brooks & Gerstoft 2007):

$$G(\mathbf{r}_\psi, \mathbf{r}_S) = \sum_{b_\psi=0}^{\infty} \Gamma^{b_\psi} G_f(L1_\psi) + \sum_{b_\psi=1}^{\infty} \Gamma^{b_\psi} G_f(L2_\psi), \qquad (2)$$

where

$$L1_\psi = \left(\sqrt{(x-x_\psi)^2 + y^2 + (2b_\psi D + z \pm z_\psi)^2} \right), \qquad (3)$$

and

$$L2_\psi = \left(\sqrt{(x-x_\psi)^2 + y^2 + (2b_\psi D - z \pm z_\psi)^2} \right). \qquad (4)$$

The symbol b_ψ represents the number of bottom bounces for a given path, D is the depth of the waveguide, the $y = 0$ horizontal axis is defined as that which contains both A and B, and $G_f(R) = \frac{e^{ikR}}{4\pi R}$ is the 3D Green's function within a homogeneous medium, where k is the wave number and R is the total distance that a particular wave travels. The first term on the RHS of Eq. (2) includes all up-going waves, and the second term includes all down-going waves as measured from the source.

Inserting Eq. (2) into Eq. (1) yields a cross-correlation expression that consists of the sum of the integrals of all possible combinations of the interaction between any path to the first receiver, and any path to the second. Consider any of these individual interactions. Substitution of Eq. (2) into Eq. (1), that is, cross-correlation between two arbitrary paths, yields (Snieder et al. 2006, Brooks & Gerstoft 2007)

$$C_{AB}(\omega) = |\rho S(\omega)|^2 n \frac{\Gamma^{b_A + b_B}}{(4\pi)^2} \iint \frac{e^{ik(L_A - L_B)}}{L_A L_B} dxdy, \qquad (5)$$

where b_ψ is the number of bottom bounces for the path to ψ, and

$$L_\psi = \sqrt{(x-x_\psi)^2 + y^2 + (2b_\psi D \pm z \pm z_\psi)^2}, \qquad (6)$$

is the length of the given path between the source, S, and receiver, ψ.

Application of the method of stationary phase to Eq. (5) (Sabra et al. 2005, Snieder et al. 2006, Bender & Orszag 1978, Brooks & Gerstoft 2007), and summation over all stationary points, yields

$$C_{AB}(\omega) = in|S(\omega)|^2 \sum_{\chi_s} \left(\frac{\Gamma^{b_A + b_B} c\rho}{2\omega \cos\theta} G_f(R(\chi_s)) \right), \qquad (7)$$

where c is the wave velocity, f is the acoustic frequency, $\omega = 2\pi f$ is the angular frequency, θ is the acute angle between the ray path and the vertical, and χ_s are the stationary points. Note that the stationary points satisfy the relationship $\theta_A = \pm\theta_B$. The positive relationship between θ_A and θ_B only occurs when the path to the furthest receiver passes through the closer receiver, hence the relationship between the summed cross-correlations and the Green's function between the receivers. The negative relationship corresponds to stationary-phase contributions from cross-correlations between a wave that initially undergoes a surface reflection, and one that does not (Sabra et al. 2005, Brooks & Gerstoft 2007). Both wave and ship sources are near the ocean surface. Thus these spurious arrivals will converge to almost the same time delay as the true Green's function

paths, and due to the long wavelengths, will not be observed as separate peaks. Hence these spurious arrivals can be neglected.

The cross-correlation in Eq. (7) produces an amplitude and phase shaded Green's function. The amplitude shading is dependent on the travel path and also contains constant and frequency dependent components. Due to the $1/\omega$ factor phase shading in Eq. (7), the time domain Green's function is proportional to the derivative of the summed cross-correlations (Roux et al. 2005, Snieder 2004, Sabra et al. 2005, Brooks & Gerstoft 2007):

$$\frac{\partial C_{AB}(t)}{\partial t} \simeq -\left[G_{AB}(t) - G_{AB}(-t)\right]. \tag{8}$$

The raw cross-correlation, rather than its time derivative, is often used as an approximation to the Green's function (Roux et al. 2004, Derode et al. 2003, Siderius et al. 2006, Gerstoft et al. 2008), and for a mid-high frequency finite bandwidth signal this can be a good approximation, since the cross-correlation and its derivative closely resemble one another. However the time-derivative, which will correct for the $\pi/2$ phase difference between the raw cross-correlation arrival peak and that of the Green's function, should be employed if exact arrival times are desired.

CROSS-CORRELATION OF ACOUSTIC DATA

Acoustic data were recorded on a 32-element L-shaped hydrophone array. The array location and geometry are shown in Figure 1.

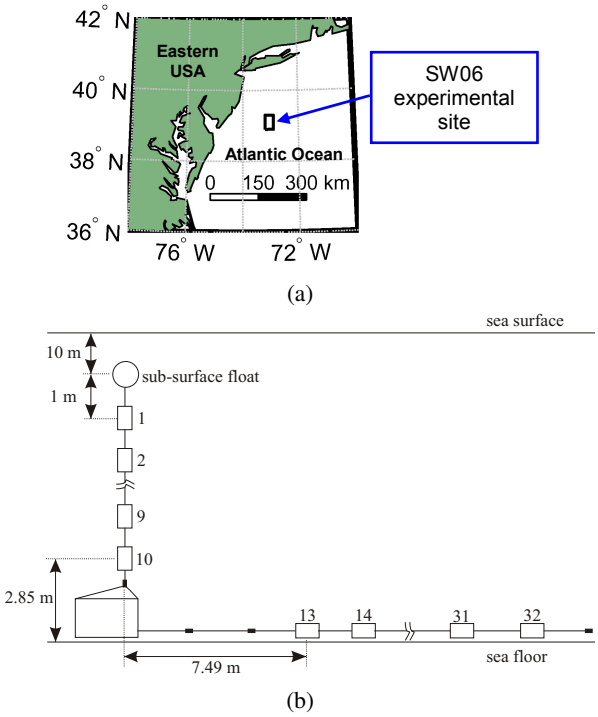

Figure 1: (a) The hydrophone array was located within the SW06 experimental site, off the Eastern coast of the USA. (b) L-shaped hydrophone array: hydrophones 1–10 represent the VLA and hydrophones 13–32 represent the HLA. Hydrophones 11–12, which were tied off at the electronics box directly underneath the VLA, are not shown.

Correlations of 20–100 Hz September 2 data recorded on the HLA and lowest VLA element of the L-shaped array were performed following the methodology outlined in the 'Cross-correlation Theory' section. Detailed empirical Green's function estimates for the data recorded on the horizontal portion of the array have been published previously (Brooks & Gerstoft 2009), and hence only a summary of the raw cross-correlation results is presented here. An example of the cross-correlations obtained between hydrophone 13 (the first hydrophone in the HLA) and all other hydrophones in the HLA is shown in Figure 2. The cross-correlations show both direct and surface-reflected paths. Although the direct-path time-distance relationship appears to the eye, to be almost linear, it is actually slightly curved. The estimated direct-path travel times in Figure 2(c) are seen to be slightly less than the simulated travel times at larger distances, suggesting that the actual length of the array is slightly less than suggested by the *a priori* geometry. In addition, differences in travel times from any given active source (at a known location) to hydrophone pairs were seen to be consistently less than expected for the assumed straight-line array geometry, suggesting that the hydrophone array may not have been located linearly on the seafloor.

INVERSION ALGORITHM FOR ARRAY ELEMENT LOCALISATION

The array element inversion process presented here approximates an array geometry with inter-hydrophone travel times that best match the measured travel time estimates. The basis for the inversion process stems from that of Sabra et al. 2005b, though the process has been adapted and modified to directly suit the array under consideration here. The bottom of the VLA is chosen as the origin, and the 20 HLA elements (hydrophones 13–32), which are all assumed to be at a constant depth, are parameterised in 2D by their distance and azimuth from the first element. The single VLA element under consideration (hydrophone 10) is parameterised by its height from the seafloor. For the purpose of the inversion, the VLA element (hydrophone 10), is denoted 'element 1', and the HLA elements, hydrophones 13–32 respectively, are denoted 'elements 2–21'.

The model vector of unknown parameters is that which defines the array geometry:

$$\mathbf{m} = [h_1, d_2, ..., d_M, \theta_2, \theta_3, ..., \theta_{M-1}]^{\mathrm{T}}, \tag{9}$$

where $M = 21$ is the number of elements (hydrophones) in the array, h_1 is the height of the VLA hydrophone above the seafloor, d_j is the distance from the origin to HLA element j, and θ_j is the azimuth relative to the two ends of the array (i.e., $\theta_M = 0$). The inversion therefore seeks to estimate $2M-2$ (i.e., 40) unknowns.

Each cross-correlation has a peak in both positive and negative time (see Figure 2), which correspond to propagation paths in opposite directions. Travel times, $T_{i,j}$, between elements i and j (for all $1 \leq i < j \leq M$), were estimated from the cross-correlated data as the mean time corresponding to the peak of the empirical Green's function approximation envelope, where 'mean' is here the average between the absolute values of the positive and negative peak times.

The observed data vector of travel times,

$$\mathbf{T} = [T_{1,2}, T_{1,3}..., T_{1,M}, T_{2,3}, ..., T_{M-1,M}]^{\mathrm{T}}, \tag{10}$$

consists of $M(M-1)/2$ (i.e., 210) terms. The array is *a priori* assumed to be straight. The *a priori* estimate of the unknown parameters is therefore $\mathbf{m_{ap}} = [l_2, ..., l_M, 0, ..., 0, c_0]^T$, where l_j is the pre-experiment measured hydrophone separation.

The inversion seeks to minimise the difference between the measured travel times and those computed from the model vector, whilst simultaneously ensuring that the resulting hydrophone locations lie on a smooth spline.

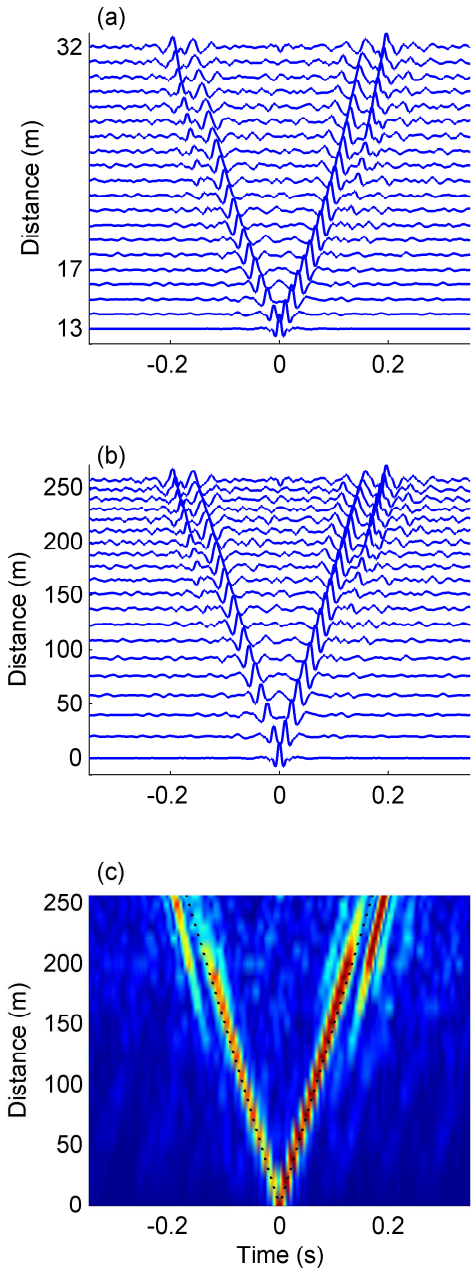

Figure 2: Cross-correlations between channel 13 (first HLA hydrophone) and all other channels plotted a) as a function of channel number, and (b) as a function of distance from Channel 13, assuming *a priori* hydrophone locations. (c) Normalised envelope of the cross-correlation function time derivative, with simulated (from *a priori* geometry) direct-path travel times (black dotted lines).

The computed travel times are

$$\mathbf{T_{cal}} = \left[\frac{\sqrt{|d_2 e^{i\theta_2}| + h_1^2}}{c_0}, ..., \frac{\sqrt{|d_k e^{i\theta_2}| + h_1^2}}{c_0}, ..., \frac{\sqrt{|d_M e^{i\theta_2}| + h_1^2}}{c_0}, \frac{|d_3 e^{i\theta_k} - d_2 e^{i\theta_j}|}{c_0}, ..., \frac{|d_k e^{i\theta_k} - d_j e^{i\theta_j}|}{c_0}, ..., \frac{|d_M e^{i\theta_M} - d_{M-1} e^{i\theta_{M-1}}|}{c_0} \right]^T. \quad (11)$$

The travel time differences should be weighted by the inverse of the uncertainties of the measured times. This is done by pre-multiplication with the diagonal regularisation matrix:

$$\mathbf{W_1} = diag\left[w_{1,2}, w_{1,3}..., w_{1,M}, w_{2,3}, ..., w_{M-1,M}\right], \quad (12)$$

where $w_{j,k}$ are uncertainty weightings for each observation data. If the uncertainty is assumed to be a constant number of samples independent of the hydrophone pair, then the difference between the observed travel times, $\mathbf{T}$, and the computed travel times, $\mathbf{T_{cal}}$, should be equally uncertain regardless of hydrophone pair. Unity regularisation weighting was therefore used.

The first objective function to be minimised is

$$\Phi_1 = [\mathbf{W_1}(\mathbf{T} - \mathbf{T_{cal}})]^T [\mathbf{W_1}(\mathbf{T} - \mathbf{T_{cal}})] \quad (13)$$

$$= [(\mathbf{T} - \mathbf{T_{cal}})]^T [(\mathbf{T} - \mathbf{T_{cal}})]. \quad (14)$$

The second consideration of the inversion is the shape of the array. The *a priori* assumption is that the array is straight. The inversion therefore seeks to minimise the difference in azimuth between straight lines connecting successive elements.

The change in azimuth vector between the lines connecting two successive elements is

$$\Delta\Theta = [\Delta\theta_2, ..., \Delta\theta_j, ..., \Delta\theta_{M-1}]^T, \quad (15)$$

where

$$\Delta\theta_j = \text{phase}(d_{j+1} e^{i\theta_{j+1}} - d_j e^{i\theta_j}) - \text{phase}(d_j e^{i\theta_j} - d_{j-1} e^{i\theta_{j-1}}). \quad (16)$$

Unity regularisation weighting is applied. The smoothness objective function is therefore

$$\Phi_2 = [\Delta\Theta]^T [\Delta\Theta]. \quad (17)$$

The objective function to be minimised is the weighted sum of Φ_1 and Φ_2:

$$\Phi = \Phi_1 + \alpha\Phi_2 = [(\mathbf{T} - \mathbf{T_{cal}})]^T [(\mathbf{T} - \mathbf{T_{cal}})] + \alpha[\Delta\Theta]^T [\Delta\Theta], \quad (18)$$

where α is the Lagrange multiplier that governs the relative importance of the observed travel times and the array smoothing.

The array geometry is estimated as that which minimises the objective function, Φ.

APPLICATION OF INVERSION ALGORITHM TO DATA

The array element localisation algorithm was applied to the travel times obtained from the September 2 ambient noise cross-correlations. Minimisation of the objective function was achieved using the MATLAB® nonlinear least squares function. The subspace trust region method for nonlinear minimisation (Celis et al. 1985, Coleman & Li 1994) was chosen over the Levenberg-Marquardt algorithm as the problem has bound constraints and is overdetermined.

Since the least-squares algorithm attempts to minimise all travel time differences, it can be susceptible to bias from outliers. The six largest values were therefore rejected for each calculation of the objective function (stability was checked and results using rejection of 5–20 largest values showed negligible variation).

Lower and upper limits on inter-element spacing were set to half and twice the *a priori* values. The large upper bound was used because inversion results yielding distances greater than the *a priori* data would have suggested a problem with either the data or the algorithm. The distances calculated from the

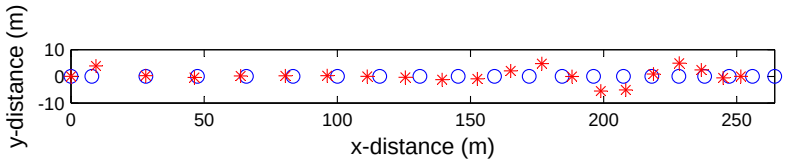

Figure 3: Array element locations: *a priori* (circles) and *a posteriori* (asterisks) results from non-linear least squares travel-time inversion.

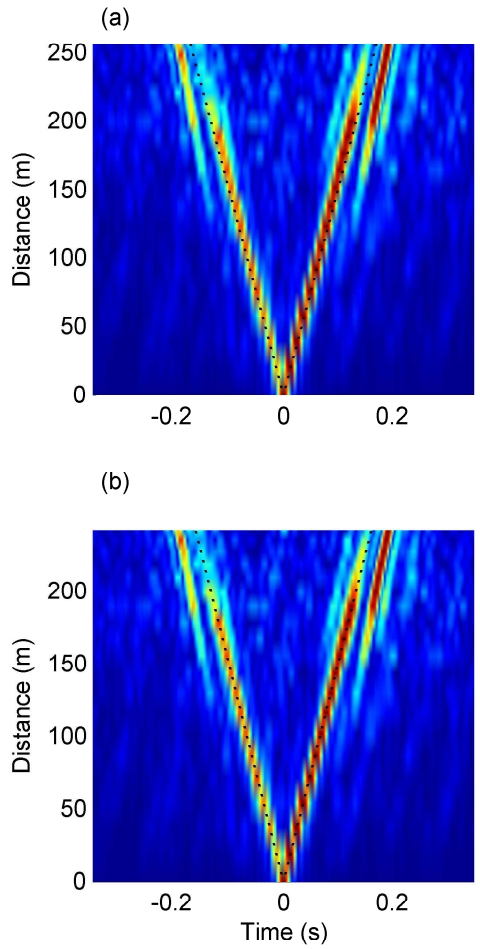

Figure 4: Normalised envelopes of the cross-correlation function time derivative, plotted as a function of distance from Channel 13 (first HLA hydrophone), with overlaid simulated direct (black dotted lines) path travel times (white dotted lines) assuming (a) the *a priori* geometry, and (b) the *a posteriori* geometry.

inversion were, however, generally about 5% less than the *a priori* values, which is consistent with the expectation that the hydrophones were spaced more closely. Different values of the Lagrange multiplier, α (see Eq. (18)), were also compared. The resulting geometry was observed to be reasonably smooth even when α was set to zero.

The inverted element location results are show in Figure 3, along with the *a priori* locations. The *a posteriori* geometry supports the original hypothesis that the HLA was not lying in a straight line. Results using estimates of the unknown parameters $\mathbf{m_{ap}}$ that are different to the *a priori* geometry converge to the same *a posteriori* geometry. The *a posteriori* geometry results yielded array spacings that better matched simulated travel times. As an example, simulated travel times are overlaid on the normalised envelopes of the cross-correlation function time derivative in Figure 4 assuming (a) the *a priori* array geometry, and (b) the *a posteriori* geometry. The *a posteriori* geometry results are seen to give a closer fit to the simulated times. Although not shown here, the *a posteriori* geometry also better matches travel times from active sources generated at known locations relative to the VLA.

CONCLUSION

Acoustic inter-hydrophone travel time estimates were extracted from ambient noise cross-correlations of hydrophone array data. These travel time estimates were successfully incorporated into an inversion algorithm for self-localisation of the horizontal portion of an L-shaped array. Inter-hydrophone travel times corresponding to the curved *a posteriori* array shape better matches simulated travel times, and also match well with travel times from active sources at known locations better than the *a priori* shape, supporting the original hypothesis that the array was not lying in a straight line

ACKNOWLEDGEMENTS

This work has been supported by the Office of Naval Research under Grant No. N00014-05-1-0264.

REFERENCES

Bender, C. M. & Orszag, S. A. 1978, *Advanced Mathematical Methods for Scientists and Engineers: Asymptotic Methods and Perturbation Theory*, McGraw-Hill.

Brekhovskikh, L. M. 1960, *Waves in layered media*, Academic Press.

Brooks, L. A. & Gerstoft, P. 2007, "Ocean acoustic interferometry", *J. Acoust. Soc. Am.* **121**(6), 3377–3385.

Brooks, L. A. & Gerstoft, P. 2009, "Green's function approximation from corss-correlations of 20-100 Hz noise during a tropical storm", *J. Acoust. Soc. Am.* **125**(2), 723–734.

Brooks, L. A., Gerstoft, P. & Knobles, D. P. 2008, "Multichannel array diagnosis using noise cross-correlation", *J. Acoust. Soc. Am. -EL* **124**, EL203–EL209.

Campillo, M. & Paul, A. 2003, "Long-range correlations in the diffuse seismic coda", *Science* **299**, 547–549.

Celis, M., Dennis, J. E. & Tapia, R. A. 1985, "A trust region strategy for nonlinear equality constrained optimization", *Numerical Optimization 1994* pp. 71–82.

Coleman, T. F. & Li, Y. 1994, "On the convergence of reflective Newton methods for large-scale nonlinear minimization subject to bounds", *Mathematical Programming* **67**(2), 189–224.

Derode, A., Larose, E., Tanter, M., de Rosny, J., Tourin, A., Campillo, M. & Fink, M. 2003, "Recovering the Green's function from field-field correlations in an open scattering medium", *J. Acoust. Soc. Am.* **113**(6), 2973–2976.

Dosso, S., Collison, N. E. B., Heard, G. J. & Verrall, R. I. 2004, "Experimental validation of regularized array element localization", *J. Acoust. Soc. Am.* **115**(5), 2129–2137.

Gerstoft, P., Hodgkiss, W. S., Siderius, M., Huang, C.-F. & Harrison, C. H. 2008, "Passive fathometer processing", *J. Acoust. Soc. Am.* **123**(3), 1297–1305.

Gerstoft, P., Sabra, K. G., Roux, P., Kuperman, W. A. & Fehler, M. C. 2006, "Green's functions extraction and surface-wave tomography from microseisms in southern California", *Geophysics* **71**(4), SI23–SI31.

Hodgkiss, W. S. 1989, Shape determination of a shallow-water bottomed array, *in* "Proc. OCEANS'89", pp. 1199–1204.

Hodgkiss, W. S., Gerstoft, P. & Murray, J. J. 2003, Array shape estimation from sources of opportunity, *in* "OCEANS 2003 Proc.".

Larose, E., Khan, A., Nakamura, Y. & Campillo, M. 2005, "Lunar subsurface investigated from correlation of seismic noise", *Geophys. Res. Lett.* **32**(16), L16201.

Lin, F., Ritzwoller, M. H., Townend, J., Bannister, S. & Savage, M. K. 2007, "Ambient noise Rayleigh wave tomography of New Zealand", *Geophys. J. Int.* **170**(2), 649–666.

Lobkis, O. I. & Weaver, R. L. 2001, "On the emergence of the Green's function in the correlations of a diffuse field", *J. Acoust. Soc. Am.* **110**(6), 3011–3017.

Loewen, M. R. & Melville, W. K. 1991, "A model of the sound generated by breaking waves", *J. Acoust. Soc. Am.* **90**(4), 2075–2080.

Malcolm, A. E., Scales, J. A. & van Tiggelen, B. A. 2004, "Extracting the Green function from diffuse, equipartitioned waves", *Phys. Rev. E.* **70**, 015601.

Roux, P., Kuperman, W. A. & the NPAL Group 2004, "Extracting coherent wave fronts from acoustic ambient noise in the ocean", *J. Acoust. Soc. Am.* **116**(4), 1995–2003.

Roux, P., Sabra, K. G., Kuperman, W. A. & Roux, A. 2005, "Ambient noise cross correlation in free space: Theoretical approach", *J. Acoust. Soc. Am.* **117**(1), 79–84.

Sabra, K. G., Conti, S., Roux, P. & Kuperman, W. A. 2007, "Passive *in vivo* elastography from skeletal muscle noise", *Appl. Phys. Lett.* **90**, 194101.

Sabra, K. G., Roux, P. & Kuperman, W. A. 2005, "Arrival-time structure of the time-averaged ambient noise cross-correlation function in an oceanic waveguide", *J. Acoust. Soc. Am.* **117**(1), 164–174.

Sabra, K. G., Roux, P., Thode, A. M., D'Spain, G., Hodgkiss, W. S. & Kuperman, W. A. 2005b, "Using ocean ambient noise for array self-localization and self-synchronization", *IEEE J. Ocean. Eng.* **30**(2), 338–347.

Shapiro, N. M., Campillo, M., Stehly, L. & Ritzwoller, M. H. 2005, "High-resolution surface-wave tomography from ambient seismic noise", *Science* **307**, 1615–1618.

Siderius, M., Harrison, C. H. & Porter, M. B. 2006, "A passive fathometer technique for imaging seabed layering using ambient noise", *J. Acoust. Soc. Am.* **120**(3), 1315–1323.

Snieder, R. 2004, "Extracting the Green's function from the correlation of coda waves: A derivation based on stationary phase", *Phys. Rev. E.* **69**(4), 046610–1–8.

Snieder, R., Wapenaar, K. & Larner, K. 2006, "Spurious multiples in seismic interferometry of primaries", *Geophysics* **71**(4), SI111–SI124.

Urick, R. J. 1975, *Principles of Underwater Sound*, McGraw-Hill, New York.

van Wijk, K. 2006, "On estimating the impulse response between receivers in a controlled ultrasonic experiment", *Geophysics* **71**(4), SI79–SI84.

Wapenaar, K. & Fokkema, J. 2006, "Green's function representations for seismic interferometry", *Geophysics* **71**(4), SI33–SI46.

Weaver, R. L. & Lobkis, O. I. 2001, "Ultrasonics without a source: Thermal fluctuation correlations at MHz frequencies", *Phys. Rev. Lett.* **87**(13), 134301–1–134301–4.

Wenz, G. M. 1962, "Acoustic ambient noise in the ocean: Spectra and sources", *J. Acoust. Soc. Am.* **34**(12), 1936–1956.

Yang, Y., Ritzwoller, M. H., Levshin, A. L. & Shapiro, N. M. 2007, "Ambient noise Rayleigh wave tomography across Europe", *Geophys. J. Int.* **168**, 259–274.